Aerodynamic Derivatives Identification Using a Non-Conservative Robust Kalman Filter

Han Sung Lee*, Won-sang Ra[†], Jang Gyu Lee*, Yongkyu Song** and Ick-Ho Whang***

Abstract – A non-conservative robust Kalman filter (NCRKF) is applied to flight data to identify the aerodynamic derivatives of an unmanned autonomous vehicle (UAV). The NCRKF is formulated using UAV lateral motion data and then compared with results from the conventional Kalman filter (KF) and the recursive least square (RLS) method. A superior performance for the NCRKF is demonstrated by simulation and real flight data. The NCRKF is especially effective in large uncertainties in vehicle modeling and in measuring flight data. Thus, it is expected to be useful in missile and aircraft parameter identification.

Keywords: Non-conservative robust Kalman filter, Aerodynamic derivatives identification, EKF, RLS

1. Introduction

Aerodynamic derivatives are an important parameter in the formulation of the dynamic equations of a vehicle in flight. They are functions of the shape of the aircraft, the control input, and the Mach number [1, 2]. To identify aerodynamic derivatives from flight data as precisely as possible, various estimation methods have been applied in the past [3-6].

These methods can be categorized into two groups of research. One formulates the aerodynamic derivatives in a linear form and estimates them using either the least square (LS) method or by the KF [7, 8]. The other method formulates the aerodynamic derivatives as augmented states, resulting in a nonlinear filtering problem. An extended Kalman filter (EKF) or a maximum likelihood (ML) method is usually employed in this problem [9-14].

The EKF and the ML methods are generally known to provide better results than the recursive least square (RLS) and the Kalman filter (KF) methods, assuming that the system and the measurements are reasonably well modeled. However, in aerodynamic derivatives identification from flight data, obtaining an acceptable model is not easy because of various uncertainties inherent in forming the dynamic equations and in the telemetering of the flight data. Based on our experience, an EKF is very sensitive to system noise covariance. A time-consuming search for the best system noise covariance, to design a filter, is thereby unavoidable. Therefore, a robust identification technique, using something other than the EKF and the ML methods, is desirable.

To avoid the limitations of a non-linear filter, a linear regression model is derived from this model. By doing this, an imperfect system noise covariance tuning is eliminated. For this regression, the aerodynamic derivatives are assumed to be constant. Therefore, the first order derivative of each state is zero.

The LS method has been used previously as identification technique for this model. However, the LS method provides an unbiased estimation under the assumption that the noise distribution is Gaussian. Unfortunately, the Gaussian assumption does not hold in the aerodynamic derivatives identification problem.

To overcome the non-Gaussian distribution problem, we propose to employ a non-conservative robust Kalman filter (NCRKF) [15-17]. The NCRKF is derived by rejecting additive noise terms in the measurement matrix to compensate for the limits of the LS and the KF methods regarding this problem.

The NCRKF was formulated to identify the aerodynamic derivatives in the lateral motion equations of an unmanned autonomous vehicle (UAV). Only the lateral motion equation was selected for simplicity. The resulting NCRKF was then compared with the RLS and the KF results to demonstrate that it performs better under inevitable modeling uncertainties. As a result, we found the NCRKF more suitable for aerodynamic derivatives identification from flight data.

2. NCRKF Formulation for UAV Lateral Motion

2.1 Dynamic equations for UAV lateral motion

Linearized lateral dynamic equations around the trim of a UAV can be expressed as [18]

---
† Corresponding Author: School of Mechanical and Control Engineering, Handong Global University, Korea (wonsang@handong.edu).
* School of Electrical Engineering, Seoul National University, Korea (ppklhs1, jgl@snu.ac.kr).
** School of Aerospace and Mechanical Engineering, Korea Aerospace University, Korea (yksong@hau.ac.kr).
*** Department of Guidance and Control, Agency for Defense Development, P.O. Box 35-11, Korea (ickho@nate.com).

$$\Delta\dot{\beta} = -\Delta r + \frac{g\Delta\phi}{U_0} + \frac{\overline{q}S}{U_0 m}C_Y, \tag{1}$$

$$\Delta\dot{p} = \frac{\overline{q}Sb_r}{I_{XX}}C_l, \tag{2}$$

$$\Delta\dot{r} = \frac{\overline{q}Sb_r}{I_{ZZ}}C_n, \tag{3}$$

$$\Delta\dot{\phi} = \Delta p, \tag{4}$$

where $\Delta\beta$ is the sideslip perturbation, Δr the yaw rate perturbation, $\Delta\phi$ the roll angle perturbation, U_0 the trim velocity of the X axis, q the aerodynamic pressure, g the gravity, m the mass, S the reference area, C_Y the aerodynamic force derivatives of the Y axis, Δp the roll rate perturbation, b_r the reference length, I_{XX} the X axis inertia, C_l the aerodynamic moment derivatives of the X axis, I_{ZZ} the Z axis inertia, and C_n the aerodynamic moment derivatives of the Z axis.

$\Delta\beta$, Δp, Δr, and $\Delta\phi$ are assumed to be measurable. In (1) ~ (3), the aerodynamic force and moment derivatives C_Y, C_l, and C_n are assumed to consist of the linear terms $\Delta\beta$, Δp, Δr, δa, and δr, where δa and δr are the aileron and the rudder inputs, respectively. They are given as [18]

$$C_Y = C_{Y_\beta}\Delta\beta + C_{Y_p}\left(\frac{b_r}{2V_m}\right)\Delta p + C_{Y_r}\left(\frac{b_r}{2V_m}\right)\Delta r + C_{Y_{\delta a}}\delta a + C_{Y_{\delta r}}\delta r, \tag{5}$$

$$C_l = C_{l_\beta}\Delta\beta + C_{l_p}\left(\frac{b_r}{2V_m}\right)\Delta p + C_{l_r}\left(\frac{b_r}{2V_m}\right)\Delta r + C_{l_{\delta a}}\delta a + C_{l_{\delta r}}\delta r, \tag{6}$$

$$C_n = C_{n_\beta}\Delta\beta + C_{n_p}\left(\frac{b_r}{2V_m}\right)\Delta p + C_{n_r}\left(\frac{b_r}{2V_m}\right)\Delta r + C_{n_{\delta a}}\delta a + C_{n_{\delta r}}\delta r, \tag{7}$$

where $V_m = \sqrt{V_X^2 + V_Y^2 + V_Z^2}$ is the total velocity.

Eqs. (5)-(7) show that the lateral dynamic UAV equations are expressed by fifteen aerodynamic derivatives. Our objective is to identify the fifteen aerodynamic derivatives from the four measurements. The aerodynamic derivatives are assumed to be constant, i.e., they are time invariant.

The above basic equations need to be formulated in different forms to be applied to the RLS, the KF, and the NCRKF methods used to identify the time invariant aerodynamic derivatives.

2.2 RLS formulation

To apply the RLS method, (1) ~ (7) are arranged in a linear regression form. It represents the fifteen aerodynamic derivatives as state variables, viz., [18]

$$\underline{x} = \begin{bmatrix} \underline{x}_1^T & \underline{x}_2^T & \underline{x}_3^T \end{bmatrix}^T,$$

$$\underline{x}_1 = \begin{bmatrix} C_{Y_\beta} & C_{Y_{\delta a}} & C_{Y_{\delta r}} & C_{Y_p} & C_{Y_r} \end{bmatrix}^T,$$
$$\underline{x}_2 = \begin{bmatrix} C_{l_\beta} & C_{l_{\delta a}} & C_{l_{\delta r}} & C_{l_p} & C_{l_r} \end{bmatrix}^T, \tag{8}$$
$$\underline{x}_3 = \begin{bmatrix} C_{n_\beta} & C_{n_{\delta a}} & C_{n_{\delta r}} & C_{n_p} & C_{n_r} \end{bmatrix}^T.$$

The aerodynamic force and moment derivatives C_Y, C_l, and C_n can then be expressed by

$$C_Y = \underline{h}^T\underline{x}_1,$$
$$C_l = \underline{h}^T\underline{x}_2, \tag{9}$$
$$C_n = \underline{h}^T\underline{x}_3,$$

where

$$\underline{h} = \begin{bmatrix} \Delta\beta & \delta a & \delta r & \left(\frac{b_r}{2V_m}\right)\Delta p & \left(\frac{b_r}{2V_m}\right)\Delta r \end{bmatrix}^T.$$

In (9), the measurement matrix is assumed to be uncorrupted by sensor noise. This is because KF and RLS use a true measurement matrix.

Now, define

$$\underline{y} = \begin{bmatrix} y_1 & y_2 & y_3 \end{bmatrix}^T,$$
$$y_1 = \frac{mU_0}{\overline{q}S}\left(\Delta\dot{\beta} + \Delta r - \frac{g\Delta\phi}{U_0}\right),$$
$$y_2 = \frac{I_{XX}}{\overline{q}Sb_r}\Delta\dot{p}, \tag{10}$$
$$y_3 = \frac{I_{ZZ}}{\overline{q}Sb_r}\Delta\dot{r}.$$

Employing the newly defined variables and introducing the measurement noises, (1)-(3) can be expressed as

$$\underline{y} = H\underline{x} + \underline{v}, \tag{11}$$

where

$$H = \begin{bmatrix} \underline{h}^T & \underline{O} & \underline{O} \\ \underline{O} & \underline{h}^T & \underline{O} \\ \underline{O} & \underline{O} & \underline{h}^T \end{bmatrix}.$$

A discrete form of (10) and (11) with sampling time T_s may be expressed as

$$\underline{y}_k = H_k\underline{x}_k + \underline{v}_k, \tag{12}$$

where

$$\underline{y}_k = \begin{bmatrix} y_{1,k} & y_{2,k} & y_{3,k} \end{bmatrix}^T, \tag{13}$$

$$y_{1,k} = \frac{mU_0}{\bar{q}_k S}\left(\frac{\Delta\beta_{k+1} - \Delta\beta_k}{T_s} + \Delta r_k - \frac{g\Delta\phi_k}{U_0} \right),$$

$$y_{2,k} = \frac{\mathrm{I}_{XX}}{\bar{q}_k Sb}\frac{\Delta p_{k+1} - \Delta p_k}{T_s},$$

$$y_{3,k} = \frac{\mathrm{I}_{ZZ}}{\bar{q}_k Sb}\frac{\Delta r_{k+1} - \Delta r_k}{T_s},$$

$$H_k = \begin{bmatrix} \underline{h}_k^T & \underline{O} & \underline{O} \\ \underline{O} & \underline{h}_k^T & \underline{O} \\ \underline{O} & \underline{O} & \underline{h}_k^T \end{bmatrix}, \tag{14}$$

$$\underline{h}_k = \begin{bmatrix} \Delta\beta_k & \delta a_k & \delta r_k & \left(\dfrac{b_r}{2V_{m,k}}\right)\Delta p_k & \left(\dfrac{b_r}{2V_{m,k}}\right)\Delta r_k \end{bmatrix}^T, \tag{15}$$

$$\underline{x}_k = \begin{bmatrix} \underline{x}_{1,k}^T & \underline{x}_{2,k}^T & \underline{x}_{3,k}^T \end{bmatrix}^T, \tag{16}$$

$$= \begin{bmatrix} \underline{x}_1^T & \underline{x}_2^T & \underline{x}_3^T \end{bmatrix}^T,$$

$$\underline{v}_k = \begin{bmatrix} v_{1,k} & v_{2,k} & v_{3,k} \end{bmatrix}^T. \tag{17}$$

Note that the state variables defined in (8) and (16) are time invariant. In other words, we want to identify constant aerodynamic derivatives.

A standard RLS algorithm can be written for (12) as [19]

$$K_k = P_{k-1}H_k^T \left(H_k P_{k-1} H_k^T + \lambda I_{3\times3} \right)^{-1}, \tag{18}$$

$$\underline{x}_k = \underline{x}_{k-1} + K_k\left(\underline{y}_k - H_k\,\underline{x}_{k-1} \right), \tag{19}$$

$$P_k = P_{k-1} - K_k H_k P_{k-1}, \tag{20}$$

where λ is a positive constant which is less than or equal to unity and P_k is the state covariance matrix.

2.3 KF formulation

To construct a system model for the KF, the state vector is defined by (16), which consists of the fifteen aerodynamic derivatives given in (8). These derivatives are assumed to be time invariant, so the system matrix is the identity matrix and the system noise is zero.

The system model can be written as

$$\underline{x}_k = I_{15\times15}\underline{x}_{k-1}, \tag{21}$$

where $I_{15\times15}$ represents the identity matrix of the 15 rows and columns.

The measurement model for the KF is the same model seen in (12). In fact, the measurement in (13) is not the sensor output, but functions of the sensor output. Therefore, it is a pseudo measurement. In this paper, pseudo measurements are not distinguished from the original meaning of measurement.

For the system and the measurement models, the KF formulation is given as [20, 21]

Time propagation

$$\hat{\underline{x}}_k^- = I_{15\times15}\hat{\underline{x}}_{k-1}^+, \tag{22}$$

$$P_k^- = I_{15\times15}P_{k-1}^+ I_{15\times15}^T, \tag{23}$$

where the system noise covariance matrix is zero because the assumption is that there is no system noise. It is therefore omitted in (23).

Measurement update

$$K_k = P_k^- H_k^T \left(H_k P_k^- H_k^T + R_k \right)^{-1}, \tag{24}$$

$$\hat{\underline{x}}_k^+ = \hat{\underline{x}}_k^- + K_k\left(\underline{y}_k - H_k\hat{\underline{x}}_k^- \right), \tag{25}$$

$$P_k^+ = \left(I - K_k H_k \right)P_k^-, \tag{26}$$

where K_k is the Kalman gain and R_k is the measurement noise covariance matrix.

2.4 NCRKF formulation

The NCRKF is the filter we use to improve estimation performance when a noise-corrupted measurement matrix is used. In (14), the noise-corrupted measurement matrix, $\tilde{H}_k$, consists of the sideslip, the roll rate, and the yaw rate sensor outputs. This means that $H_{T,k}$ can be expressed in its measurement and error terms as

$$H_{T,k} = \tilde{H}_k - H_{E,k}, \tag{27}$$

where

$$H_{T,k} = \begin{bmatrix} \underline{h}_{T,k}^T & \underline{O} & \underline{O} \\ \underline{O} & \underline{h}_{T,k}^T & \underline{O} \\ \underline{O} & \underline{O} & \underline{h}_{T,k}^T \end{bmatrix}, \tag{28}$$

$$\underline{h}_{T,k} = \begin{bmatrix} \Delta\beta_{T,k} & \delta a_{T,k} & \delta r_{T,k} & \left(\dfrac{b_r}{2V_{m,k}}\right)\Delta p_{T,k} & \left(\dfrac{b_r}{2V_{m,k}}\right)\Delta r_{T,k} \end{bmatrix}^T, \tag{29}$$

$$H_{E,k} = \begin{bmatrix} \underline{h}_{E,k}^T & \underline{O} & \underline{O} \\ \underline{O} & \underline{h}_{E,k}^T & \underline{O} \\ \underline{O} & \underline{O} & \underline{h}_{E,k}^T \end{bmatrix}, \tag{30}$$

$$\underline{h}_{E,k} = \begin{bmatrix} \Delta\beta_{E,k} & \delta a_{E,k} & \delta r_{E,k} & \left(\dfrac{b_r}{2V_{m,k}}\right)\Delta p_{E,k} & \left(\dfrac{b_r}{2V_{m,k}}\right)\Delta r_{E,k} \end{bmatrix}^T, \tag{31}$$

$$\Delta\beta_{T,k} = \Delta\tilde{\beta}_k - \Delta\beta_{E,k}, \tag{32}$$

$$\Delta p_{T,k} = \Delta\tilde{p}_k - \Delta p_{E,k}, \tag{33}$$

$$\Delta r_{T,k} = \Delta\tilde{r}_k - \Delta r_{E,k}, \tag{34}$$

$$\delta a_{T,k} = \delta\tilde{a}_k - \delta a_{E,k}, \tag{35}$$

$$\delta r_{T,k} = \delta\tilde{r}_k - \delta r_{E,k}. \tag{36}$$

The subscripts T and E mean true and error, respectively.

The KF and the RLS methods use the same measurement matrix corrupted by inevitable sensor noise found in (27). Unfortunately, the KF and the RLS methods have no algorithm that compensates for a noise-corrupted measurement matrix, resulting in poor estimation performance.

The NCRKF is designed to eliminate this measurement matrix error. The cost function of the NCRKF contains measurement matrix error, whereas that of the KF does not consider it. By minimizing the cost function, the NCRKF provides two correction terms that eliminate this error. The NCRKF formulation is a modified KF formulation that adds these correction terms [15]. In other words, without the correction terms, the NCRKF becomes equivalent to the KF.

In a previous study, the NCRKF had good results with regard to estimation accuracy and fast convergence [15, 16]. The other benefit of the NCRKF is that the noise distribution does not need to be Gaussian. Its distribution is restricted to zero mean white.

The NCRKF also has the same system and measurement models as the KF. The NCRKF formulation is given as [15]

Time propagation

$$\hat{\underline{x}}_k^- = I_{15\times15}\hat{\underline{x}}_{k-1}^+ , \qquad (37)$$

$$P_k^- = I_{15\times15}P_{k-1}^+ I_{15\times15}^T . \qquad (38)$$

Measurement update

$$P_k^+ = \left(\left(P_k^-\right)^{-1} + \tilde{H}_k^T R_k^{-1}\tilde{H}_k - W_k\right)^{-1} , \qquad (39)$$

$$\begin{aligned}\hat{\underline{x}}_k^+ &= \left(I + P_k^+ W_k\right)\hat{\underline{x}}_k^- \\ &+ P_k^+\tilde{H}_k^T R_k^{-1}\left(y_m - \tilde{H}_k^T\hat{\underline{x}}_k^-\right) - P_k^+\underline{V}_k\end{aligned} , \qquad (40)$$

where $E\left[H_{E,k}\right] = 0$.

In (39) ~ (40), the correction terms are present, which are defined by

$$W_k = E\left[H_{E,k}^T R_k^{-1} H_{E,k}\right] , \qquad (41)$$

$$\underline{V}_k = E\left[H_{E,k}^T R_k^{-1}\underline{v}_k\right] . \qquad (42)$$

The W_k and the $\underline{V}_k$ calculations are explained later. Providing proper R_k and $\underline{V}_k$ is important. Using (12), (13), (17), and (32)~(36), the measurement noise and the measurement noise covariance matrix can be written as

$$\underline{v}_k = \begin{bmatrix} v_{1,k} & v_{2,k} & v_{3,k} \end{bmatrix}^T , \qquad (43)$$

where

$$v_{1,k} = \frac{mU_0}{\overline{q}_k S}\left(\frac{\Delta\beta_{E,k+1} - \Delta\beta_{E,k}}{T_s} + \Delta r_{E,k} - \frac{g\Delta\phi_{E,k}}{U_0}\right),$$

$$v_{2,k} = \frac{I_{XX}}{\overline{q}_k Sb_r}\frac{\Delta p_{E,k+1} - \Delta p_{E,k}}{T_s},$$

$$v_{3,k} = \frac{I_{ZZ}}{\overline{q}_k Sb_r}\frac{\Delta r_{E,k+1} - \Delta r_{E,k}}{T_s},$$

$$R = E\left[\underline{v}_k\underline{v}_k^T\right] = \begin{bmatrix} R_{11} & 0 & R_{13} \\ 0 & R_{22} & 0 \\ R_{31} & 0 & R_{33} \end{bmatrix}, \qquad (44)$$

$$R_{11} = \left(\frac{mU_0}{S}\right)^2\left[\frac{2}{T_s^2}E\left[\frac{\Delta\beta_{E,k}^2}{\overline{q}_k^2}\right] + E\left[\frac{\Delta r_{E,k}^2}{\overline{q}_k^2}\right] + \frac{g^2}{U_0^2}E\left[\frac{\Delta\phi_{E,k}^2}{\overline{q}_k^2}\right]\right],$$

$$R_{13} = R_{31} = -\left(\frac{mU_0 I_{ZZ}}{S^2 b_r}\right)\left(\frac{1}{T_s}E\left[\frac{\Delta r_{E,k}^2}{\overline{q}_k^2}\right]\right),$$

$$R_{22} = \left(\frac{I_{XX}}{Sb_r}\right)^2\left[\frac{2}{T_s^2}E\left[\frac{\Delta p_{E,k}^2}{\overline{q}_k^2}\right]\right],$$

$$R_{33} = \left(\frac{I_{ZZ}}{Sb_r}\right)^2\left[\frac{2}{T_s^2}E\left[\frac{\Delta r_{E,k}^2}{\overline{q}_k^2}\right]\right].$$

Using (30), (31), (43), and (44), the correction terms in (41) and (42) are derived as

$$\begin{aligned}W_k &= E\left[H_{E,k}^T R_k^{-1} H_{E,k}\right] \\ &= \begin{bmatrix} R_{11,k}^{-1}E\left[\underline{h}_{E,k}\underline{h}_{E,k}^T\right] & 0_{5\times5} & R_{13,k}^{-1}E\left[\underline{h}_{E,k}\underline{h}_{E,k}^T\right] \\ 0_{5\times5} & R_{22,k}^{-1}E\left[\underline{h}_{E,k}\underline{h}_{E,k}^T\right] & 0_{5\times5} \\ R_{31,k}^{-1}E\left[\underline{h}_{E,k}\underline{h}_{E,k}^T\right] & 0_{5\times5} & R_{33,k}^{-1}E\left[\underline{h}_{E,k}\underline{h}_{E,k}^T\right] \end{bmatrix}\end{aligned}, \qquad (45)$$

$$\underline{V}_k = \begin{bmatrix} -R_{11,k}^{-1}\frac{mU_0}{S}\frac{1}{T_s}E\left[\frac{\Delta\beta_{E,k}^2}{\overline{q}_k}\right] \\ \underline{0}_{3\times1} \\ R_{11,k}^{-1}\frac{mU_0}{S}\left(\frac{b_r}{2V_{m,k}}\right)E\left[\frac{\Delta r_{E,k}^2}{\overline{q}_k}\right] - R_{13,k}^{-1}\frac{I_{ZZ}}{Sb_r}\frac{1}{T_s}\left(\frac{b_r}{2V_{m,k}}\right)E\left[\frac{\Delta r_{E,k}^2}{\overline{q}_k}\right] \\ \underline{0}_{3\times1} \\ -R_{22,k}^{-1}\frac{I_{XX}}{Sb_r}\frac{1}{T_s}\left(\frac{b_r}{2V_{m,k}}\right)E\left[\frac{\Delta p_{E,k}^2}{\overline{q}_k}\right] \\ \underline{0}_{1\times1} \\ -R_{31,k}^{-1}\frac{mU_0}{S}\frac{1}{T_s}E\left[\frac{\Delta\beta_{E,k}^2}{\overline{q}_k}\right] \\ \underline{0}_{3\times1} \\ R_{31,k}^{-1}\frac{mU_0}{S}\left(\frac{b_r}{2V_{m,k}}\right)E\left[\frac{\Delta r_{E,k}^2}{\overline{q}_k}\right] - R_{33,k}^{-1}\frac{I_{ZZ}}{Sb_r}\frac{1}{T_s}\left(\frac{b_r}{2V_{m,k}}\right)E\left[\frac{\Delta r_{E,k}^2}{\overline{q}_k}\right] \end{bmatrix}, \qquad (46)$$

where

$$E\left[\underline{h}_{E,k}\,\underline{h}_{E,k}^{T}\right]$$

$$=\begin{bmatrix} E\left[\Delta\beta_{E,k}^{2}\right] & 0 & 0 & 0 & 0 \\ 0 & E\left[\delta a_{E,k}^{2}\right] & 0 & 0 & 0 \\ 0 & 0 & E\left[\delta r_{E,k}^{2}\right] & 0 & 0 \\ 0 & 0 & 0 & \left(\dfrac{b_r}{2V_{m,k}}\right)^{2}E\left[\Delta p_{E,k}^{2}\right] & 0 \\ 0 & 0 & 0 & 0 & \left(\dfrac{b_r}{2V_{m,k}}\right)^{2}E\left[\Delta r_{E,k}^{2}\right] \end{bmatrix}.$$

With these calculations, the NCRKF expressed in (37)-(40) is complete.

3. Simulation and Aerodynamic Derivatives Identification Using Flight Data

3.1 Simulation

The new identification method using the NCRKF is first verified through simulation. All simulation data are generated to be analogous to UAV flight data. Fig. 1 shows a UAV; its specifications are given in Table 1. This UAV was built by the Flight Control Laboratory of Korea Aerospace University in Korea. The UAV was engaged in formation flight to produce flight data to be utilized in aerodynamic derivatives identification.

Fig. 1. UAV

Table 1. UAV Specification

Characteristics	Value (unit)
Mass	11.74 (kg)
Wing area	1.06 (m^2)
Wing span	2.5 (m)
Inertia (I$_{XX}$, I$_{YY}$, I$_{ZZ}$)	1.3, 3.5, 2.5 (kg m^2)

Fig. 2 shows the aileron and the rudder inputs applied in the flight test. After 12 seconds, there are no maneuvers. These data are also used in simulation.

For the noise-corrupted measurement matrix in (30), the sensor noise is determined by considering the standard deviation of the sensor. The sensor bias is not considered because the NCRKF, as well as the RLS and the KF, does
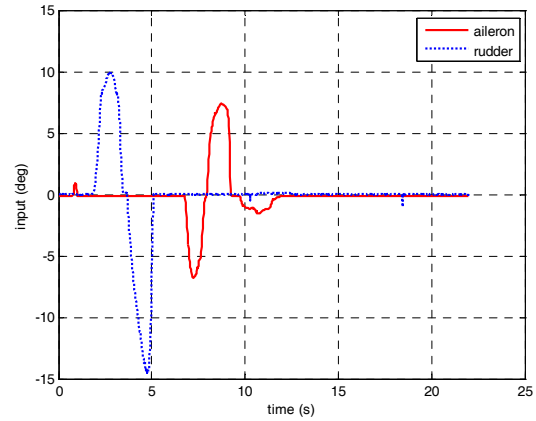

Fig. 2. Aileron and Rudder Inputs (deg)

Table 2. Sensor Noise (simulation)

Sensor	Standard deviation (unit)
Sideslip	1 (deg)
Roll rate	0.2 (deg/s)
Yaw rate	0.2 (deg/s)
Roll angle	1 (deg)

not have any algorithm to eliminate the sensor bias term. In this simulation, we focus on verifying the estimation performance of each method under the assumption that the sensor bias has been removed. The standard deviation of the sensor is given in Table 2.

To verify the proposed method, the Monte-Carlo simulation is carried out 100 times. All true values are assumed to be known, so the estimation error of aerodynamic derivatives and trajectory error are calculated exactly. The initial state was given using twice the true aerodynamic derivatives. The aerodynamic derivatives were then determined using the RLS, the KF, and the NCRKF methods.

As seen in Figs. 3-6, the sideslip, the roll rate, the yaw rate, and the roll angle trajectories show that the estimation performance of the NCRKF is remarkably superior to the RLS and the KF methods. This is because the NCRKF has an algorithm that eliminates the inevitable measurement matrix error given in (30). Within twelve seconds, the NCRKF shows fast convergence as well as good estimation accuracy. After twelve seconds, all trajectories, except for the roll angle, converge to the true trajectory because the aileron and the rudder inputs are zero, as seen in Fig. 2.

In Fig. 6, the roll angle trajectories determined by the KF and the RLS methods have a big bias error compared with the NCRKF. This is because they are obtained by the integration of an incorrect roll rate estimate.

Table 3 shows the trajectory error, which is obtained by the average absolute error in each Monte-Carlo trial. The NCRKF shows the best estimation performance, which is remarkably superior. The accuracy of the KF is better than that of the RLS in all but the roll angle error.

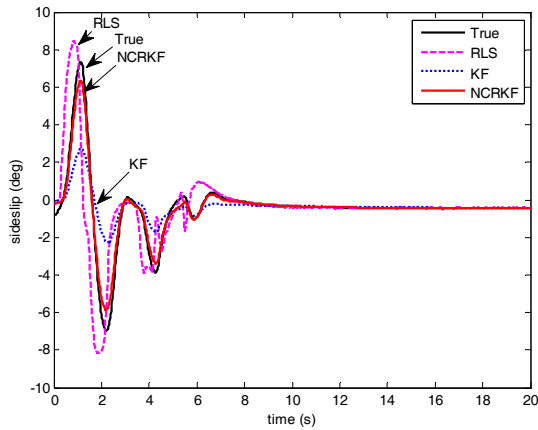Table 4 gives the derivatives estimated by each method.
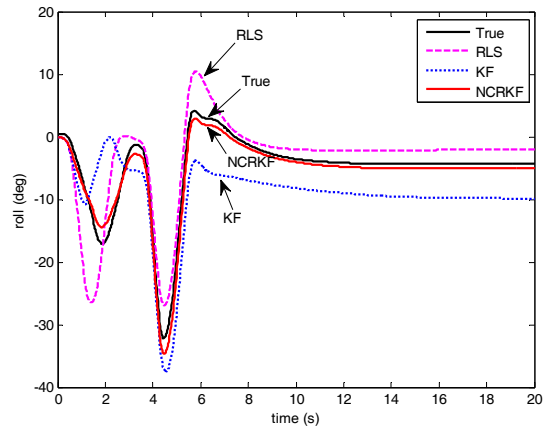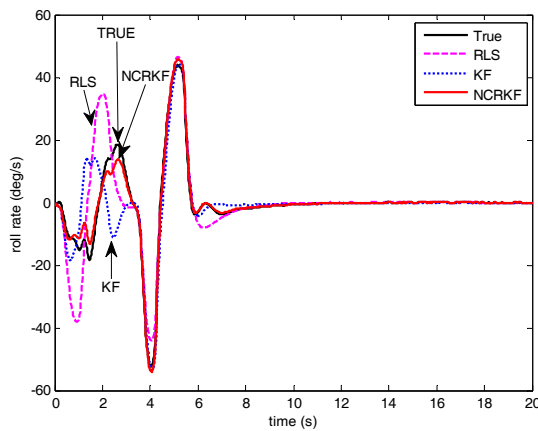
Fig. 3. Sideslip (deg)

Fig. 4. Roll Rate (deg/s)

Fig. 5. Yaw Rate (deg/s)

The NCRKF has a greatly superior estimation performance compared with the RLS and the KF methods. The RLS and the KF methods show a similar estimation performance except in the force derivatives.

Regarding the force derivatives, the KF performs better than the RLS. This is because the RLS has a weakness in the sideslip error differential term in (13). If the sideslip error is close to zero in the simulation, the RLS has a

Fig. 6. Roll Angle (deg)

Table 3. Trajectory Error Comparison (Simulation)

Method	Sideslip error (deg)	Roll rate error (deg/s)	Yaw rate error (deg/s)	Roll angle error (deg)
RLS	0.684	3.306	2.296	3.142
KF	0.504	2.867	1.948	5.580
NCRKF	0.133	0.657	0.424	0.918

similar performance as the KF.

Table 4 illustrates that the NCRKF eliminates the measurement matrix error found in (30) efficiently. The moment derivatives of the NCRKF are close to the true derivatives. The force derivatives from the NCRKF have a small error compared with the RLS and the KF methods.

Table 4. Aerodynamic Derivatives Estimation (The initial states are twice the true values.)

Derivatives	True	RLS	KF	NCRKF
C_{Y_β}	-0.902	-23.38	-6.415	-1.823
$C_{Y_{\delta a}}$	-0.358	18.41	-0.659	-0.695
$C_{Y_{\delta r}}$	-0.041	23.18	-0.079	-0.081
C_{Y_p}	0.273	-19.36	0.538	0.549
C_{Y_r}	0.561	88.80	1.116	1.115
C_{l_β}	-0.013	-0.006	-0.006	-0.011
$C_{l_{\delta a}}$	0.083	0.076	0.076	0.079
$C_{l_{\delta r}}$	-0.034	-0.041	-0.041	-0.036
C_{l_p}	-0.184	-0.173	-0.173	-0.176
C_{l_r}	-0.218	-0.243	-0.243	-0.225
C_{n_β}	0.051	0.028	0.028	0.048
$C_{n_{\delta a}}$	-0.058	-0.033	-0.033	-0.051
$C_{n_{\delta r}}$	-0.038	-0.017	-0.017	-0.036
C_{n_p}	0.115	0.083	0.083	0.104
C_{n_r}	-0.129	-0.053	-0.054	-0.124

3.2 Aerodynamic derivatives identification using flight data

Using flight data from a UAV, aerodynamic derivatives identification has also been conducted. The initial state is taken from the estimate made with the RLS method, under the assumption that there is no information about initial aerodynamic derivatives. The initial estimate of the RLS is obtained through the LS method.

To evaluate the performance of each method, the trajectory derived by a dynamic equation is compared with the measured trajectory. This is because we do not know the true aerodynamic derivatives. Although the measurement is not true, its error is bounded by the sensor characteristics.

The theoretical R_k obtained from the standard deviations given in Table 2 is used in flight data. The NCRKF also performs better than the RLS and the KF, as shown in Table 5.

Table 5. Trajectory Error Comparison (Flight Data)

Method	Sideslip error (deg)	Roll rate error (deg/s)	Yaw rate error (deg/s)	Roll angle error (deg)
RLS	2.686	10.35	31.23	70.91
KF	2.699	10.42	31.38	71.26
NCRKF	1.623	6.666	24.34	50.45

To obtain improved identification performance for flight data, the R_k given in Table 2 has to be adjusted. This is because uncertainties, such as sensor bias or control input error, might exist. These have a bad effect on the estimation performance of filters.

The R_k tuning method is simple. The standard deviation candidates of the sideslip are arbitrarily selected as follows: [0.01:0.01:0.1] [0.2:0.1:5] [5:0.2:10] [11:1:15]. Those of the roll rate and the yaw rate are [0.0001:0.0001:0.001] [0.001:0.001:0.01] [0.01:0.01:0.1] [0.2:0.1:1] [1.5:0.5:10] [11:1:15]. Each number of a square bracket indicates [initial number:increment:final number] and the unit is degree or degree per second.

The simulation is carried out 345960 times and the standard deviation with minimum trajectory error is selected for R_k. The standard deviations of sideslip, roll rate, and yaw rate given in Table 2 are changed to 3, 0.05, and 15, respectively. After R_k tuning, the performance of NCRKF is more improved than that of NCRKF without tuning. As a result, the errors of sideslip, roll rate, yaw rate, and roll angle given in Table 3 are reduced to 0.774, 6.330, 5.295, and 6.957, respectively.

From Figs. 7 to 10, the trajectories of sideslip, roll rate, yaw rate, and roll angle show that the estimation performance of the NCRKF is greatly improved after 12 seconds, compared with the RLS and the KF methods. Through the scheme that eliminates measurement matrix error corrupted by inevitable sensor noise, the estimation
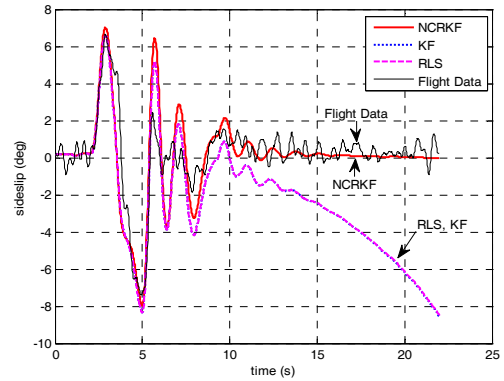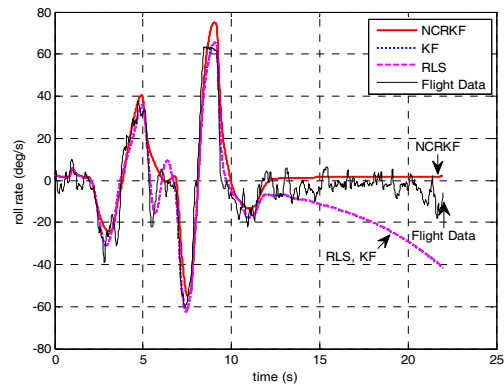

Fig. 7. Sideslip (deg)
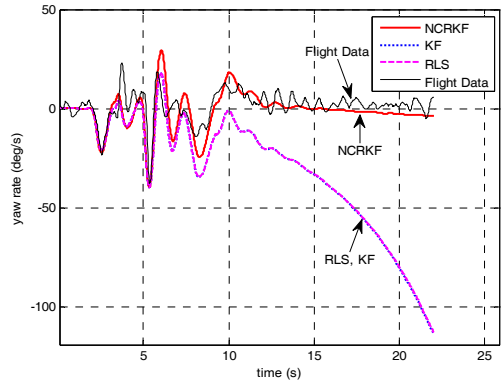

Fig. 8. Roll rate (deg/s)
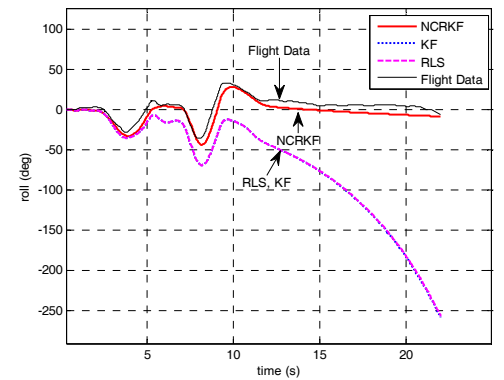

Fig. 9. Yaw rate (deg/s)

Fig. 10. Roll angle (deg)

performance of the proposed method is also verified for real flight data. Note that the performance of the RLS and the KF methods is similar to each other in all of the figures. This is because the initial state of the KF is determined by the RLS estimate.

The contributions of this paper are summarized as follows. The proposed method overcomes the limitation of nonlinear identification problem, such as augmented state structure and system noise covariance tuning, which cause performance degradation.

Through flight data, as well as simulation, the proposed method provides the feasibility of identification using flight data from the view point of robustness and accuracy of estimate.

4. Conclusion

In this paper, a new aerodynamic derivatives identification method, using the NCRKF, is proposed. To avoid the imperfect system noise covariance tuning found in EKF, the dynamic equation is changed to a linear regression form, and is used for the measurement model.

To verify the proposed method, the identification methods, using NCRKF, RLS, and KF, were carried out for simulation and flight data. The sensor data of sideslip, roll rate, yaw rate, and roll angle are used for the measurements, resulting in the measurement matrix being corrupted by inevitable sensor noise. In terms of this inevitable measurement matrix error, the NCRKF can compensate for the error efficiently, whereas conventional representative identification methods do not have a viable correction scheme.

Regarding the aerodynamic derivatives identification using flight data as well as simulation, the proposed method demonstrates a more superior accuracy and robustness compared with conventional RLS and KF methods. We conclude that the proposed method is suitable for aerodynamic derivatives identification using flight data.

Acknowledgments

References

[1] Brain L. Stevens, Frank L. Lewis, *Aircraft Control and Simulation*. John Wiley and Sons, Inc., 2003, ch. 2.

[2] P. G. Hamel and R. Jategaonkar, "Evolution of flight vehicle system identification," *J. Aircraft*, 1996, 33, (1), pp. 9-28.

[3] M. R. Ananthasayanam, "Parameter Estimation of a Flight Vehicle Using MMLE/BFGS Estimator Under Limited Measurements," *AIAA Paper 02-4624*, August, 2002.

[4] T. J. Sooy, "Aerodynamic Predictions, Comparisons, and Validations Using Missile DATCOM (97) and Aeroprediction 98 (AP98) ," *AIAA Paper 04-1246*, January, 2004.

[5] G. Chowdhary, "Aerodynamic Parameter Estimation from Flight Data Applying Extended and Unscented Kalman Filter," *AIAA Paper 06-6146*, August, 2006.

[6] S. Singh, "Parameter Estimation from Flight Data of a missile using Maximum Likelihood and Neural Network Method," *AIAA Paper 06-6284*, August, 2006.

[7] Y. Song and B. Song, "A Comparative Study of Real-Time Aircraft Parameter Identification Schemes Applied to NASA F/A-18 HARV Flight Data," *Transactions of the Japan Society for Aeronautical and Space Sciences*, Vol. 45, No. 149, 2002.

[8] Y. Song, B. Seanor, M. Napolitano, G. Campa, "Online Parameter Estimation Techniques Comparison Within a Fault Tolerant Flight Control System," *Journal of Guidance, Control, and Dynamics*, Vol. 25, No. 3, 2002

[9] J.G. Lee and D. H. Lee, "Aerodynamic Parameter Identification of a Tactical Missile Utilizing Post flight Telemetry Data," *AIAA 12th Atmospheric Flight Mechanics Conference*, Snowmass, Colorado, August 1985.

[10] H. Y. Yang, *Aerodynamic Parameter Identification of a Missile using Maximum Likelihood Method and Extended Kalman Filter*, MS. Dissertation, Department of Electrical Engineering and The Graduate School of Seoul National University, 1984.

[11] T. G. Sung, *Missile Aerodynamic Parameter Identification under Uncertain Model Structure*, MS. Dissertation, Department of Electrical Engineering and The Graduate School of Seoul National University, 1986.

[12] D. H. Lee, *Comparison of Parameter Identification Algorithms for an Aircraft*, Ph.D. Dissertation, Department of Electrical Engineering and The Graduate School of Seoul National University, 1992.

[13] S. T. Park, J.G. Lee and G. Chen, "Comments on 'Modified Extended Kalman Filtering and a Real-Time Parallel Algorithm for System Parameter Identification," *IEEE Transactions on Automatic Control*, Vol. 40, No. 9, September 1995, pp. 1661-1662.

[14] Y. Song and M.S. Hwang, "A Study on the Aircraft Parameter Estimation form Flight Test Data," *Journal of the KSAS*, Vol. 26, No. 6, October, 1998, pp. 1-12.

[15] W. S. Ra, I. H. Whang, and J. B. Park, "Non-conservative robust Kalman filtering using a noise corrupted measurement matrix", *IET Control Theory and Applications*, 2009, Vol. 3, Iss. 9, pp. 1226–1236.

[16] W. S. Ra, *Non conservative Robust Kalman Filtering Using Noise Corrupted Measurement Matrix*, Ph.D. Dissertation, Department of Electrical and Electronic Engineering and The Graduate School of Younsei University, December 2008.

[17] I. H. Whang, W. S. Ra, and J. Y. Ahn, "A modified weighted least squares range estimator for ASM (anti-ship missile) application," *Int. Journal of Control, Automation, and Systems*, 2005, 3, (3), pp. 486-492.

[18] Robert C. Nelson, *Flight Stability and Automatic Control, 2nd Ed.*, McGraw Hill, 1998.

[19] Simon Haykin, *Adaptive filter theory*, Prentice Hall, Upper Saddle River, New Jersey 070458, 2002.

[20] A. Gelb (ed.), *Applied optimal estimation*, Cambridge, MA: MIT press, 1974.

[21] F. L. Lewis, *Optimal estimation: with an introduction to stochastic control theory*, New York: John Wiley & Sons, 1986.

Han Sung Lee received his B.S. degree in Electrical Engineering from the Han Yang University in 2002. He is currently a Ph.D. candidate at the Seoul National University. His research interests include inertial navigation system, filtering theory, and aerodynamic coefficient identification.

Won-Sang Ra received his B.E. degree in Electrical Engineering and his M.S. degree in Electrical and Computer Engineering, as well as his Ph.D. degree in Electrical and Electronics Engineering, from Yonsei University, Seoul, Korea, in 1998, 2000, and 2009, respectively. From March 2000 to February 2009, he was with the Guidance and Control Department of the Agency for Defense Development, Daejeon, as a Senior Researcher. Since March 2009, he has been with the School of Mechanical and Control Engineering, Handong Global University, where he is currently an Assistant Professor. His main research topics include the robust filtering theory and its applications to autonomous vehicle guidance and control.

Jang Gyu Lee is a professor at the Department of Electrical Engineering, Seoul National University (SNU), Seoul, Korea since 1982. He received his B.S. degree in Electrical Engineering from SNU in 1971, and his M.S. and Ph.D. degrees from the University of Pittsburgh, Pittsburgh, PA, in 1974, and 1977, respectively. His research interests include navigation, and guidance and control in various applications.

Yongkyu Song is a professor at the School of Aerospace and Mechanical Engineering, Korea Aerospace University, Kyonggido, Korea. His research interests include system identification of flight vehicles, control of unmanned aerial vehicles, and flight tests.

Ick-Ho Whang received his B.S., M.S., and Ph.D. degrees in Control and Instrumentation Engineering from Seoul National University, Seoul, Korea, in 1988, 1990, and 1995, respectively. Since 1995, he has worked with the Agency for Defense Development, Daejeon, Korea as a principal researcher. His research interests include missile guidance and control, filtering theory and application, and target tracking filter.